

Supporting information

## Visible light photoexcitation of pyridine surface complex leading to selective dehydrogenative cross-coupling with cyclohexane

Shimpei Naniwa,<sup>a</sup> Akira Yamamoto<sup>a,b</sup> and Hisao Yoshida<sup>\*a,b</sup>

<sup>a</sup> *Department of Interdisciplinary Environment, Graduate School of Human and Environmental Studies, Kyoto University, Yoshida Nihonmatsu-cho, Sakyo-ku, Kyoto 606-8501, Japan*

<sup>b</sup> *Elements Strategy Initiative for Catalysts & Batteries (ESICB), Kyoto University, Kyotodaigaku Katsura, Nishikyo-ku, Kyoto 615-8520, Japan*

\* E-mail address: yoshida.hisao.2a@kyoto-u.ac.jp

### Contents

<b>1. Optimization of the photocatalyst</b> .....	2
<b>1.1. Titanium oxide</b> .....	2
<b>1.2. Metal cocatalyst</b> .....	2
<b>2. Bond dissociation energy (BDE)</b> .....	3
<b>3. UV-vis spectroscopy</b> .....	4
<b>4. Control experiments</b> .....	5
<b>5. Calculation of free energy changes</b> .....	6
<b>References</b> .....	6

## 1. Optimization of the photocatalyst

### 1.1. Titanium oxide

The reaction tests were carried out with various Pt(0.1)/TiO<sub>2</sub> samples for the dehydrogenative cross-coupling (DCC) reaction under visible light irradiation ( $\lambda > 422$  nm). The results are shown in Table S1. Among these catalysts, the Pt(0.1)/JRC-TIO-8 sample (Table S1, entry 1, ST-01, anatase, 338 m<sup>2</sup> g<sup>-1</sup>) and the Pt(0.1)/JRC-TIO-6 sample (Table S1, entry 2, rutile, 100 m<sup>2</sup> g<sup>-1</sup>) showed high activity and selectivity. Among the two, the former gave a less amount of cyclohexanone and cyclohexanol than the latter, leading to the higher selectivity to CHPs based on cyclohexane ( $S_{Cy} = 91\%$ ). JRC-TIO-4 and JRC-TIO-2 (Table S1, entries 3 and 4), which have lower specific surface area, provided less active photocatalysts than JRC-TIO-8 and JRC-TIO-6. Therefore, we employed JRC-TIO-8 as the TiO<sub>2</sub> photocatalyst in the following experiments.

**Table S1** Results of the reaction tests under photoirradiation with various Pt(0.1)/TiO<sub>2</sub> photocatalysts <sup>a</sup>

Entry	TiO <sub>2</sub>	Crystal phase	Specific surface area / m <sup>2</sup> g <sup>-1</sup>	Products / $\mu\text{mol}^b$				Selectivity (%) <sup>c</sup>	
				CHPs	BPs	BCH	CHOs	$S_{Py}$	$S_{Cy}$
1	JRC-TIO-8	Anatase	338	1.2	0.11	0.011	0.098	83	91
2	JRC-TIO-6	Rutile	100	1.2	0.058	0.038	0.27	91	78
3	JRC-TIO-4	Anatase, rutile	50	0.46	0.042	0.015	0.24	85	63
4	JRC-TIO-2	Anatase	8	0	0	0	0.25	-	-

<sup>a</sup> Reaction conditions: pyridine (0.10 mL, 1.2 mmol) and cyclohexane (1.9 mL, 18 mmol) with the Pt(0.1)/TiO<sub>2</sub> photocatalyst (0.1 g) were used, the reaction time was 2 h, the light intensity was 130 mW cm<sup>-2</sup> measured at  $395 \pm 35$  nm in wavelength, and the irradiation wavelength was  $\lambda > 422$  nm. <sup>b</sup> CHPs: total amount of 2-CHP, 3-CHP, and 4-CHP. BPs: total amount of 2,2'-BP, 2,3'-BP, and 2,4'-BP. CHOs: total amount of cyclohexanone and cyclohexenol. <sup>c</sup> DCC selectivity based on pyridine was calculated as:  $S_{py} = [100 \times \text{CHPs} (\mu\text{mol})] / [(\text{CHPs} + 2 \times \text{BPs}) (\mu\text{mol})]$ ; DCC selectivity based on cyclohexane as:  $S_{cy} = [100 \times \text{CHPs} (\mu\text{mol})] / [(\text{CHPs} + 2 \times \text{BHC} + \text{CHOs}) (\mu\text{mol})]$ .

### 1.2. Metal cocatalyst

Next, we examined some kinds of metal co-catalyst on the TiO<sub>2</sub> (JRC-TIO-8) photocatalyst for the DCC reaction under visible light irradiation ( $\lambda > 400$  nm, Table S2). Generally, it is considered that metal co-catalyst on photocatalysts can suppress the recombination of the photogenerated electrons and holes.<sup>S1-3</sup> The Pt loaded photocatalyst (Table S2, entry 2) showed higher activity than the non-metal loaded photocatalyst (Table S2, entry 1). This suggests that the loaded Pt species actually worked as a charge separator to enhance the photocatalytic activity. Among various metal loaded catalysts (Table S2, entries 3–5), the Pt loaded catalyst showed the best activity and selectivity (Table S2, entry 3). Interestingly, a Pd loaded sample promoted the homo-coupling of pyridine rather than the cross-coupling while Pt and Rh loaded samples showed similarly good activities toward the cross-coupling. Since we previously reported that Pd co-catalyst on TiO<sub>2</sub> can activate benzene ring for the addition of photogenerated radicals in several photocatalytic reactions,<sup>S4-7</sup> it can be assumed that pyridine, one of heteroaromatics, is also activated by Pd co-catalyst to promote its homo-coupling through the radical addition-elimination mechanism.

Also, we optimized the loading amount of Pt on the photocatalyst (Table S3). Decreasing the loading amount from 0.1 wt% did not affect so much the amount of the cross-coupling products but it increased the amount of by-products such as cyclohexanone and cyclohexanol (Table S3, entries 1–3). This indicates that more surface hydroxyl groups were exposed with decreasing the loading amount of Pt and this could enhance the photocatalytic oxidation of cyclohexane.<sup>S2</sup> On the other hand, the cross-coupling yield was decreased with increasing the loading amount from 0.1 wt% (Table S3,

entries 5 and 6). This might be due to a variation of the particle size or the number of Pt nanoparticles deposited on the TiO<sub>2</sub> surface.

Finally, according to these results shown in Figs. S1, S2, and S3, the Pt(0.1)/TIO-8 was employed as the best catalyst.

**Table S2** Results of the reaction tests under photoirradiation with various M(0.1)/TiO<sub>2</sub> photocatalysts <sup>a</sup>

Entry	Metal	Products / $\mu\text{mol}^b$				Selectivity (%) <sup>b</sup>	
		CHPs	BPs	BCH	CHOs	$S_{\text{Py}}$	$S_{\text{Cy}}$
1	-	1.3	0.080	0.12	0.31	89	70
2	Pt	3.5	0.27	0.47	0.18	87	76
3 <sup>c</sup>	Pt	4.4	6.2	0.029	0.084	26	97
4 <sup>c</sup>	Rh	4.0	6.8	0.029	0.15	23	95
5 <sup>c</sup>	Pd	1.7	9.3	0	0.22	8.0	88

<sup>a</sup> Reaction conditions: pyridine (1.2 mmol) and cyclohexane (18 mmol) with the M(0.1)/TIO-8 photocatalyst (0.1 g) were used, the reaction time was 2 h, the light intensity was 130 mW cm<sup>-2</sup> measured at 395  $\pm$  35 nm in wavelength, and the irradiation wavelength was  $\lambda > 400$  nm. <sup>b</sup> See the caption of Table S1. <sup>c</sup> Pyridine (12 mmol) and cyclohexane (9.3 mmol) were used.

**Table S3** Results of the reaction tests under photoirradiation with various Pt(x)/TiO<sub>2</sub> photocatalysts <sup>a</sup>

Entry	$x$ (wt%)	Products / $\mu\text{mol}^b$				Selectivity (%) <sup>b</sup>	
		CHPs	BPs	BCH	CHOs	$S_{\text{Py}}$	$S_{\text{Cy}}$
1	0.001	1.4	0.0048	0.061	0.36	99	74
2	0.01	1.4	0.0092	0.058	0.35	99	75
3	0.025	1.7	0.0059	0.053	0.15	99	87
4	0.1	1.5	trace	0.041	0.020	>99	94
5	0.2	1.0	0	0.019	0.0067	>99	96
6	0.5	0.68	trace	0.013	0.087	>99	86

<sup>a</sup> Reaction conditions: pyridine (0.31 mmol) and cyclohexane (18 mmol) with the Pt(x)/TIO-8 photocatalyst (0.1 g) were used, the reaction time was 2 h, the light intensity was 160 mW cm<sup>-2</sup> measured at 395  $\pm$  35 nm in wavelength, and the irradiation wavelength was  $\lambda > 422$  nm. <sup>b</sup> See the caption of Table S1.

## 2. Bond dissociation energy (BDE)

Some C–H Bond dissociation energies (BDEs) for pyridine and cyclohexane reported in literature are summarized in Table S4.

**Table S4** C–H Bond dissociation energies of pyridine and cyclohexane <sup>a</sup>

Compound	Site	BDE / kJ mol <sup>-1</sup>
Pyridine	2	439.3 $\pm$ 0.8
	3	468.6 $\pm$ 8.4
	4	468.6 $\pm$ 8.4
Cyclohexane	-	416.3

<sup>a</sup> The values were cited from ref. S<sup>8</sup>.

### 3. UV-vis spectroscopy

UV-visible absorption spectra of pyridine and cyclohexane were measured in a transmission mode using a UV-vis spectrophotometer (JASCO V-570). For a measurement of the absorption spectrum of pyridine, 1.0  $\mu\text{L}$  of pyridine was dissolved in 5.0 mL of cyclohexane. The obtained spectra are shown in Fig. S1. Pyridine showed an absorption band up to 300 nm (Fig. S1a), while cyclohexane did no absorption (Fig. S1b).

Diffuse reflectance UV-vis spectra were recorded in the manner described in the main text. The pyridine adsorbed  $\text{TiO}_2$  sample exhibited a large absorption band (Fig. S2b), while the spectrum of the cyclohexane adsorbed sample was almost same with that of the  $\text{TiO}_2$  sample itself (Figs. S2a and S2c).

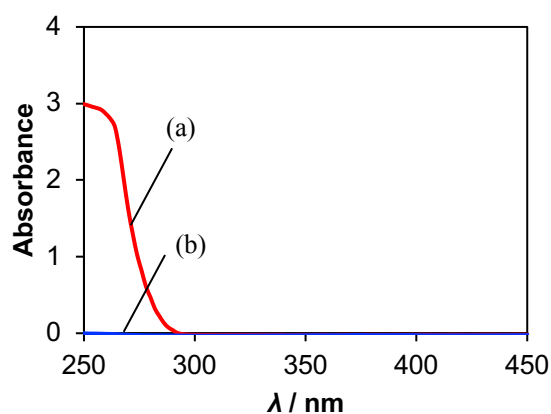


**Fig. S1** Absorption spectra of pyridine (a) and cyclohexane (b) recorded in a transmission mode. Pyridine was diluted by cyclohexane solvent.

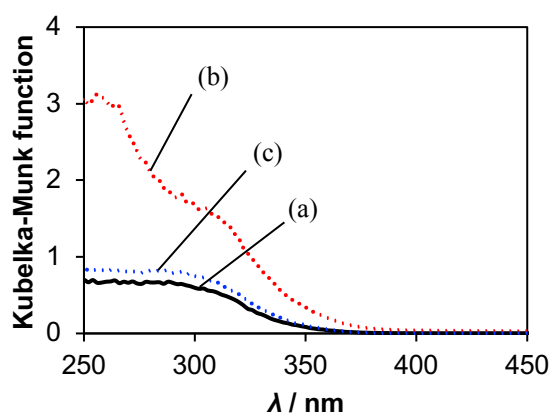


**Fig. S2** Diffuse reflectance UV-vis spectra of the  $\text{BaSO}_4$  diluted  $\text{TiO}_2$  sample (a), that with pyridine (b), and that with cyclohexane (c).

#### 4. Control experiments

To compare the hole oxidation reactivity of pyridine and that of cyclohexane, the reaction tests were carried out with neat pyridine, neat cyclohexane, and a 1:1 mixture of them (Table S5). When the reaction was carried out with neat pyridine or cyclohexane, the amount of homo-coupling products, BPs and BCH, were 51 and 40  $\mu\text{mol}$ , respectively (Table S5, entries 1 and 2). These results show that the rates of the hole oxidation to these molecules are almost similar, *i.e.*, it is only 1.2 times faster for the hole oxidation of pyridine. When the reaction was carried out with a 1:1 mixture of pyridine and cyclohexane (Table S5, entry 3), the amount of the homo-coupling products from cyclohexane (BCH) was 1.5  $\mu\text{mol}$ , which was much lower than that in the reaction without pyridine shown in Table S5, entry 2. On the other hand, the amount of the homo-coupling products from pyridine (BPs) was 31  $\mu\text{mol}$ , which was slightly lower than that in the reaction without cyclohexane shown in Table S5, entry 1. Therefore, it can be concluded that pyridine is preferentially oxidized than cyclohexane in their mixture, *i.e.*, the holes are more easily consumed by the pyridine oxidation. This would originate from that the larger amount of pyridine is adsorbed on the  $\text{TiO}_2$  surface by the acid-base interaction.

**Table S5** Results of the photocatalytic reaction tests with neat pyridine, neat cyclohexane, and a mixture of them <sup>a</sup>

Entry	Substrate	Products / $\mu\text{mol}$ <sup>b</sup>			
		CHPs	BPs	BCH	CHO
1 <sup>c</sup>	Pyridine	0	51	0	0
2 <sup>d</sup>	Cyclohexane	0	0	40	0.11
3 <sup>e</sup>	Pyridine (50%) + Cyclohexane (50%)	10	31	1.5	0.23

<sup>a</sup> Reaction conditions: the Pt(0.1)/TiO-14 photocatalyst (50 mg) was used, the reaction time was 1 h, the light intensity was  $160 \text{ mW cm}^{-2}$  measured at  $395 \pm 35 \text{ nm}$  in wavelength, and the irradiation wavelength was  $\lambda > 350 \text{ nm}$ . <sup>b</sup> See the caption of Table S1. <sup>c</sup> Pyridine (12 mmol) was used. <sup>d</sup> Cyclohexane (9.3 mmol) was used. <sup>e</sup> Pyridine (5.3 mmol) and cyclohexane (5.3 mmol) were used.

## 5. Calculation of free energy changes

Changes of free energy ( $\Delta G^\circ$ ) in the reactions of the pyridine radical cation ( $C_5H_5N^{+\bullet}$ ) with pyridine ( $C_5H_5N$ ) and that with cyclohexane ( $C_6H_{12}$ ), and a deprotonation of the cation radical were estimated (eqs. 1–3 in the main text). The Gibbs energy in the C–H bond dissociation of pyridine and cyclohexane were calculated to be 406 and 383  $\text{kJ mol}^{-1}$ , respectively, where the values were given from the BDEs in pyridine and cyclohexane (439.3 for site 2 and 416.3  $\text{kJ mol}^{-1}$ , respectively, listed in Table S4) minus the entropy factor ( $T\Delta S$ , taken in all the cases as 33  $\text{kJ mol}^{-1}$  at 298 K).<sup>S9,10</sup> The oxidation potential of H<sup>•</sup> to H<sup>+</sup> was  $-1.87$  V (vs SCE) in acetonitrile,<sup>S9,10</sup> which is the same for the two reactions. The one electron oxidation potential of pyridine was 1.82 V (vs Ag/Ag<sup>+</sup>),<sup>S11</sup> which is also the same. The energy diagrams of these calculations were shown in Fig. S3, and the  $\Delta G^\circ$  values in the reactions of pyridine radical cation with pyridine and cyclohexane, and the deprotonation were calculated to be  $-28$  and  $-51$ , and  $-28$   $\text{kJ mol}^{-1}$ , respectively. They are all thermodynamically favorable exergonic reactions, and the reaction of the pyridine radical cation ( $C_5H_5N^{+\bullet}$ ) with cyclohexane ( $C_6H_{12}$ ) were the most favorable (eq. 2 in the main text).

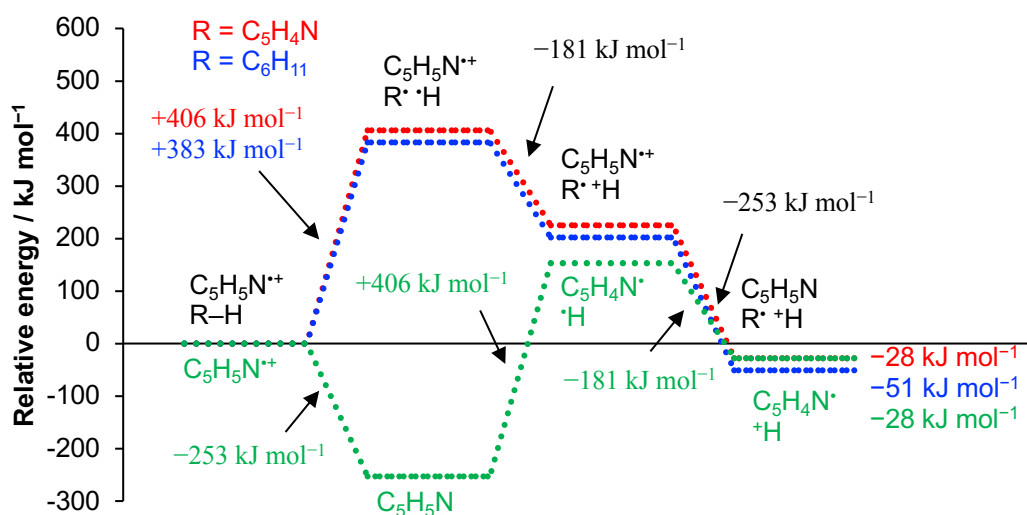


Fig. S3 Energy diagram used for the calculation of the Gibbs energy changes.

## References

- S1 C. M. Wang, A. Heller and H. Gerischer, *J. Am. Chem. Soc.*, 1992, **114**, 5230–5234.  
 S2 V. Subramanian, E. E. Wolf and P. V. Kamat, *J. Am. Chem. Soc.*, 2004, **126**, 4943–4950.  
 S3 J. Yang, D. Wang, H. Han and C. Li, *Acc. Chem. Res.*, 2013, **46**, 1900–1909.  
 S4 H. Yoshida, Y. Fujimura, H. Yuzawa, J. Kumagai and T. Yoshida, *Chem. Commun.*, 2013, **49**, 3793–3795.  
 S5 A. Tyagi, T. Matsumoto, T. Kato and H. Yoshida, *Catal. Sci. Technol.*, 2016, **6**, 4577–4583.  
 S6 E. Wada, T. Takeuchi, Y. Fujimura, A. Tyagi, T. Kato and H. Yoshida, *Catal. Sci. Technol.*, 2017, **7**, 2457–2466.  
 S7 A. Yamamoto, T. Ohara and H. Yoshida, *Catal. Sci. Technol.*, 2018, **8**, 2046–2050.  
 S8 Y. R. Ruo, *Handbook of Bond Dissociation Energies in Organic Compounds*, CRC Press, 2002.  
 S9 E. Baciocchi, T. Del Giacco and F. Elisei, *J. Am. Chem. Soc.*, 1993, **115**, 12290–12295.  
 S10 E. Baciocchi, T. Del Giacco, O. Lanzalunga, P. Mencarelli and B. Procacci, *J. Org. Chem.*, 2008, **73**, 5675–5682.  
 S11 N. L. Weinberg and H. R. Weinberg, *Chem. Rev.*, 1968, **68**, 449–523.